0026-895X/06/7004-1281–1290
MOLECULAR PHARMACOLOGY
U.S. Government work not protected by U.S. copyright
*Mol Pharmacol* 70:1281–1290, 2006

Vol. 70, No. 4
26294/3138132
*Printed in U.S.A.*



# Regulation of Mouse Hepatic α-Amino-β-Carboxymuconate-ε-Semialdehyde Decarboxylase, a Key Enzyme in the Tryptophan-Nicotinamide Adenine Dinucleotide Pathway, by Hepatocyte Nuclear Factor 4α and Peroxisome Proliferator-Activated Receptor α

Mariko Shin,[1] Insook Kim, Yusuke Inoue,[2] Shioko Kimura, and Frank J. Gonzalez

*Laboratory of Metabolism, National Cancer Institute, National Institutes of Health, Bethesda, Maryland*

Received May 3, 2006; accepted June 28, 2006

## ABSTRACT

Nicotinamide adenine dinucleotide (NAD) plays a critical role in the maintenance of cellular energy homeostasis. α-Amino-β-carboxymuconate-ε-semialdehyde decarboxylase (ACMSD) is the key enzyme regulating de novo synthesis of NAD from L-tryptophan (Trp), designated the Trp-NAD pathway. *Acmsd* gene expression was found to be under the control of both hepatocyte nuclear factor 4α (HNF4α) and peroxisome proliferator-activated receptor α (PPARα). Constitutive expression of ACMSD mRNA levels were governed by HNF4α and down-regulated by activation of PPARα by the ligand Wy-14,643 ([4-chloro-6-(2,3-xylidino)-2-pyrimidinylthio]acetic acid]), as revealed by studies with hepatic HNF4α-null mice and PPARα-null mice, respectively. Transient transfection and electrophoretic mobility shift analyses showed an HNF4α binding site in the *Acmsd* gene promoter that directed transactivation of reporter gene constructs by HNF4α. The *Acmsd* promoter was not responsive to PPARα in transactivation assays. Wy-14,643 treatment decreased HNF4α protein levels in wild-type, but not PPARα-null, mouse livers, with no changes in HNF4α mRNA. These results show that Wy-14,643, through PPARα, post-transcriptionally down-regulates HNF4α protein levels, leading to reduced expression of the HNF4α target gene *Acmsd*.

Nicotinamide adenine dinucleotide (NAD) plays a critical role as a cofactor for oxidation-reduction enzymes and histone deacetylase, and as a substrate for second messenger cADP-ribose production and poly(ADP-ribosylation). Exposure to xenobiotic chemicals can result in altered total pyridine nucleotide levels, notably decreases in NAD caused by increased degradation or decreased biosynthesis of NAD; at the extreme, this can lead to apoptosis and cell death. The biosynthesis of NAD is under tight regulation by two routes in mammalian livers: de novo synthesis from L-tryptophan (Trp) and from nicotinic acid (see Fig. 1).

α-Amino-β-carboxymuconate-ε-semialdehyde (ACMS), generated from 3-hydroxyanthranilic acid and catalyzed by 3-hydroxyanthranilic acid oxygenase, is metabolized by α-amino-β-carboxymuconate-ε-semialdehyde decarboxylase (ACMSD) (E.C.4.1.1.45) or nonenzymatically to quinolinic acid, which is finally converted to NAD by quinolinate phosphoribosyltransferase (QAPRT) (E.C.2.4.2.19). ACMSD activity is found in the liver and kidney, although the activity in liver is much lower than that in kidney (Ikeda et al., 1965). On the other hand, L-Trp 2,3-dioxygenase (TDO) (E.C.1.13.11.11), the enzyme that initiates the Trp-NAD

This work was supported by the National Cancer Institute Intramural Research Program.

[1] Current affiliation: School of Pharmacy, Kobe-Gakuin University, Nishi-ku, Kobe, 651-2180, Japan.

[2] Current affiliation: Faculty of Engineering, Gunma University, Gunma, Japan.

Article, publication date, and citation information can be found at http://molpharm.aspetjournals.org.
doi:10.1124/mol.106.026294.

**ABBREVIATIONS:** NAD, nicotinamide adenine dinucleotide; Trp, L-tryptophan; ACMS, α-amino-β-carboxymuconate-ε-semialdehyde; ACMSD, α-amino-β-carboxymuconate-ε-semialdehyde decarboxylase; QAPRT, quinolinate phosphoribosyltransferase; TDO2, L-tryptophan 2,3-dioxygenase; PP, peroxisome proliferator(s); PPARα, peroxisome proliferator-activated receptor α; PUFA, polyunsaturated fatty acids; HNF4α, hepatocyte nuclear factor 4α; PPARα$^{-/-}$, PPARα-null mice; PPARα$^{+/+}$, PPARα wild-type mice; HNF4α$^{F/F}$, HNF4α-floxed mice; HNF4α$^{\Delta L}$, liver-specific HNF4α-null mice; PCR, polymerase chain reaction; OTC, ornithine transcarbamylase; GAPDH, glyceraldehyde-3-phosphate dehydrogenase; RACE, rapid amplification of 5′-cDNA end; ACOX1, peroxisomal acyl-CoA oxidase; bp, base pair; EMSA, electrophoretic mobility shift assay(s); PPRE, peroxisome-proliferator responsive element; L-PK, liver-type pyruvate kinase; apoC-III, apolipoprotein C-III; RXRα, retinoic X receptor α; DR1, hexanucleotide direct repeat 1; Wy-14,643, [4-chloro-6-(2,3-xylidino)-2-pyrimidinylthio]acetic acid; AMPK, AMP-activated protein kinase.

pathway, is only detectable in liver. Therefore, in mammals, liver is the sole organ having the complete Trp-NAD pathway, and hepatic ACMSD and QAPRT play critical roles in NAD biosynthesis, especially in the case of restricted niacin availability (Bender, 1983).

Several steps of NAD biosynthesis from Trp have been reported to be up- or down-regulated by various factors, including hormones (Mehler et al., 1958), nutrients (Sanada and Miyazaki, 1984; Egashira et al., 2004), and drugs (Shin et al., 1999); however, the molecular mechanisms governing these changes are largely unknown. Clofibrate, a hypolipidemic drug that stimulates peroxisome proliferation and fatty acid β-oxidation, significantly increases hepatic NAD and total pyridine nucleotide levels in rats (Loo et al., 1995; Shin et al., 1999). From the study of Trp fluxes in rat liver, the Trp-NAD pathway was increased by decreasing the flux via the glutarate pathway in hepatocytes prepared from rats fed a clofibrate diet (Shin et al., 1996). The activities of key enzymes such as ACMSD and QAPRT changed in concert with the increase in hepatic NAD (Shin et al., 1999). Peroxisome proliferators (PP) such as Wy-14,643, plasticizer phthalate esters, and dehydroepiandrosterone showed the same effect on ACMSD and QAPRT activities as clofibrate (Shin et al., 1999). Because most of these drugs are known activators of peroxisome proliferator-activated receptor α (PPARα), a member of the nuclear receptor superfamily, the possibility exists that expression of the *Acmsd* and *Qaprt* genes are regulated by PPARα. PPARα is predominantly expressed in liver, heart, and kidney, which are tissues that carry out fatty acid oxidation.

Because the present study revealed that only ACMSD mRNA was down-regulated by activation of PPARα, it was examined in detail in the present study. The molecular mechanism for regulation of *Acmsd* by PPARα is not known. *Acmsd* is transcriptionally down-regulated by dietary polyunsaturated fatty acids (PUFA) (Egashira et al., 2004). Expression of many other genes is also regulated by PUFA, for which PPARα-dependent or -independent mechanisms have been proposed (Jump et al., 1999; Jump, 2002; Pegorier et al., 2004). Fatty acyl-CoA, putative endogenous PPARα ligands, are associated with hepatocyte nuclear factor 4α (HNF4α) (Hertz et al., 2001; Petrescu et al., 2002; Hostetler et al., 2005), another member of the nuclear receptor superfamily that is expressed in the liver, kidney, intestine, and pancreas (Sladec and Seidel, 2001). In mammalian liver, HNF4α functions as a homodimer and plays an important role in regulating genes involved in gluconeogenesis (Rhee et al., 2003), ureagenesis (Inoue et al., 2002), coagulation (Inoue et al., 2006a), amino acid synthesis (Kamiya et al., 2004), and bile acid synthesis (Inoue et al., 2006b).

The current study was initiated to determine whether PP affects Trp-NAD metabolism through altering the expression or activity of ACMSD and whether this regulation is mediated by PPARα and/or HNF4α. The results revealed that HNF4α directly activates the *Acmsd* gene by binding to a specific binding site located in the promoter, whereas PPARα reduces *Acmsd* expression by suppressing HNF4α protein levels.

## Materials and Methods

**Animals.** PPARα-null mice and liver-specific HNF4α-null mice used in this study were as described previously (Lee et al., 1995; Hayhurst et al., 2001). The PPARα-null mice and their controls were of a 129/Sv genetic background, whereas the liver-specific HNF4α-null mice and their littermate controls were of mixed 129/Sv, C57BL/6, FVB genetic background. Six-week-old PPARα-null mice ($PPAR\alpha^{-/-}$) and their littermates ($PPAR\alpha^{+/+}$) or 45-day-old male mice with $HNF4\alpha^{flox/flox}$ without the albumin-Cre transgene ($HNF4\alpha^{F/F}$) and $HNF4\alpha^{flox/flox}$ with the albumin-Cre transgene ($HNF4\alpha^{\Delta L}$) were housed in a pathogen-free facility under standard 12-h light/dark cycle with water and diet ad libitum. Experiments were carried out in accordance with animal study protocols approved by the National Cancer Institute, Animal Care and Use Committee.

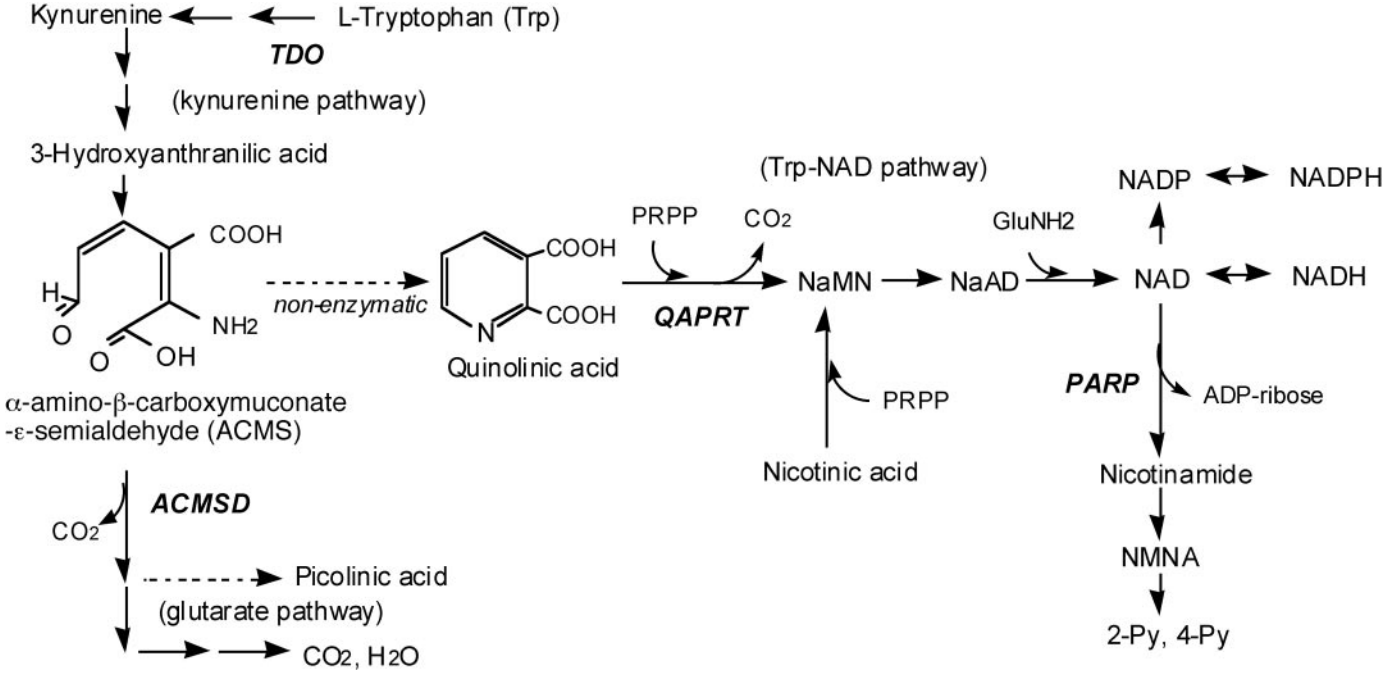


**Fig. 1.** Metabolic pathway of Trp-NAD biosynthesis in mammalian liver. NAD is biosynthesized by catalysis of QAPRT from quinolinic acid that is formed nonenzymatically from ACMS. ACMS is produced from Trp and completely oxidized through the glutarate pathway by ACMSD.

Diets containing 0.1% (w/w) Wy-14,643 were prepared by Bioserv (Frenchtown, NJ) and fed to mice ad libitum for 3 days (HNF4α mice) or 2 weeks (PPARα mice). Livers were removed, weighed, quick-frozen in liquid nitrogen, and stored at −80°C until analysis.

**Crude Enzyme Preparation and Measurement of Enzyme Activity.** A 25% liver homogenate was prepared using a Polytron homogenizer in 50 mM potassium phosphate buffer, pH 7.0, containing 140 mM potassium chloride, 5 mM 2-mercaptoethanol, 1 mM dithiothreitol, 1 mM EDTA, and 1 mM phenylmethylsulfonyl fluoride. The homogenate was centrifuged at 105,000*g* for 1 h at 4°C, and the supernatant was used for the determination of ACMSD activity. ACMSD activity was determined by the decrease in absorbance at 360 nm that monitors the decrease of ACMS produced from 3-hydroxyanthranilic acid. 3-Hydroxyanthranilic acid oxygenase was partially purified from acetone powder of mouse liver and used for the assay of ACMSD (Mehler, 1956). The BCA Protein Assay Kit (Pierce, Rockford, IL) was used to measure total protein content.

**Reverse-Transcription and Real-Time Polymerase Chain Reaction.** Total RNA (2 μg) prepared from each mouse liver with TRIzol reagent (Invitrogen, Carlsbad, CA) was reverse-transcribed in a final volume of 40 μl of first-strand buffer including oligo(dT) primer and SuperScript II Reverse Transcriptase (Invitrogen). For real-time polymerase chain reaction (PCR) analyses of reverse-transcribed cDNA, 1 μl of product was used as template with specific primers for each gene and SYBR Green PCR Master Mix (Applied Biosystems, Foster City, CA), and analysis was done with an ABI PRISM, 7900HT Sequence Detection System (Applied Biosystems). The PCR conditions were 95°C for 10 min, followed by 40 cycles of 15 s at 95°C and 60 s at 60°C. Serial dilution of each PCR product was used to draw a standard curve, and mRNA levels were determined and normalized for ribosomal protein 36B4.

**Northern Blot Analysis.** Hepatic total RNA (10 μg) was fractionated by electrophoresis on a 1% agarose gel containing 0.7% formaldehyde and transferred to GeneScreen Plus membranes (DuPont, Wilmington, DE). Blots were hybridized at 65°C with [$^{32}$P]dCTP labeled cDNA probes generated by random primer labeling kit (Ready-To-Go DNA labeling beads; Amersham Biosciences, Piscataway, NJ) in PerfectHyb Plus hybridization buffer (Sigma, St. Louis, MO). After washing, blots were exposed to a PhosphorImager screen, followed by visualization of signal using a Molecular Dynamics Storm 860 PhosphorImager system (Molecular Dynamics, Sunnyvale, CA). cDNA used as a probe were amplified from a mouse hepatic cDNA library using gene-specific primers, which were then cloned into the pCR TOPOII vector (Invitrogen). The sequence was confirmed by sequencing with a CEQ 2000XL DNA Analysis system and CEQ 2000 Dye Terminator cycle sequencing kit (Beckman Coulter, Fullerton, CA).

**Western Blot Analysis.** Frozen livers were gently homogenized in a glass tube with a manual pestle, and nuclear and cytoplasmic extracts were prepared using NE-PER nuclear and cytoplasmic extraction reagents (Pierce), with the addition of proteinase inhibitors (Roche inhibitor mixture set I and 1 mM phenylmethylsulfonyl fluoride). Nuclear or cytoplasmic protein (15–50 μg) was subjected to SDS-polyacrylamide gel electrophoresis (10–12.5%), followed by transfer to a polyvinylidene difluoride membrane (Amersham Biosciences). The membrane was incubated with phosphate-buffered saline containing 0.1% Tween 20 and 5% dry milk for 1 h and then overnight with a primary antibody against HNF4α (dilution 1:500) (Santa Cruz Biotechnology, Santa Cruz, CA), HMGB1 (dilution 1:3000) (gift from Michael Bustin, National Cancer Institute), ornithine transcarbamylase (OTC) (dilution 1:3000) (gift from Masataka Mori, Japan), or glyceraldehyde-3-phosphate dehydrogenase (GAPDH) (dilution 1:20,000) (gift from Kyung Lee, National Cancer Institute). After washing, the membrane was incubated with a 1:5000 diluted peroxidase-conjugated secondary antibody (Santa Cruz Biotechnology), and the product was visualized using a chemiluminescent system (Super Signal West Pico Chemiluminescent Substrate; Pierce). The gels were scanned, and the bands were quantified by analysis of tagged image files using Image/J 1.36b software (Research Services Branch, National Institute of Mental Health, National Institutes of Health). The HMGB1 and GAPDH signals were used as loading controls for quantifying expression of HNF4α and OTC proteins, respectively.

**Determination of the Transcription Start Site of *Acmsd*.** The transcription start site of the mouse *Acmsd* gene was determined using mouse liver total RNA and the rapid amplification of 5′-cDNA end (RACE) method with the GeneRacer Kit (Invitrogen). After first-strand cDNA synthesis, PCR was performed with GeneRacer 5′-primer and a reverse gene-specific primer located within *Acmsd* exon 1. To generate a gene-specific RACE PCR product, nested PCR was performed with GeneRacer 5′-nested primer and reverse gene-specific nested primer. The transcription start site was determined by sequencing cloned PCR products.

**Construction of Mouse ACMSD-Luciferase Reporter Plasmids and Site-Directed Mutagenesis.** The −685, −295, −220, and −52/+66 fragments from the transcription start site of the mouse *Acmsd* gene were amplified by PCR using a common ACMSD-specific 3′-primer and a 5′-primer and cloned into the luciferase reporter vector, pGL3-basic (Promega, Madison, WI). Mutations were introduced into the HNF4α-response element in the ACMSD-luciferase constructs (−685 and −295) using PCR-based, site-directed mutagenesis with QuikChange Site-Directed Mutagenesis Kit (Stratagene, La Jolla, CA). All of the plasmids were confirmed by DNA sequencing.

**Cell Culture and Transient Transfection Assay.** HepG2 or CV-1 cells were cultured in Dulbecco's modified Eagle's medium (BioSource, Camarillo, CA) containing 10% fetal bovine serum (Gemini Bio-products, Woodland, CA) and 100 units/ml antibiotics/antimycotic (Invitrogen). For transfection, cells were grown to 80 to 90% confluence in 24-well tissue culture plates without antibiotics. Transfection was performed using Lipofectamine 2000 (Invitrogen) with Opti-MEM I according to the manufacturer's instruction with ACMSD reporter constructs (500 ng/well), plasmid pRL/TK (Promega) containing the *Renilla* luciferase gene as an internal control (100 ng/well), and expression vectors pSG5/HNF4α, pCMV/rHNF1α, pSG5/mPPARα, or pSG5/hRXRα (20, 100, or 150 ng each/well). After incubation for 4 to 5 h at 37°C, medium was changed to Dulbecco's modified Eagle's medium containing fetal bovine serum and antibiotics and subsequently cultured for 40 to 44 h. Cells were then washed with phosphate-buffered saline, and the lysates were prepared using Dual-Luciferase Reporter Assay System (Promega) according to the manufacturer's instruction. Luciferase activity was determined using Monolight 3010 Luminometer (BD Biosciences PharMingen, San Diego, CA), and the relative luciferase activity was expressed as a -fold induction based on the activity of pGL3-basic.

**Electrophoretic Mobility Shift Assay.** Nuclear extracts were prepared from livers of PPARα$^{+/+}$, PPARα$^{-/-}$, HNF4α$^{F/F}$, and HNF4α$^{\Delta L}$ mice fed control or Wy-14,643 diet. Nuclear extract (5 μg) was preincubated at room temperature for 20 min in 20 mM HEPES-KOH, pH 7.9, 60 mM KCl, 0.3 mM $MgCl_2$, 0.5 mM EDTA, 1.5 μg of poly(dI-dC), 10% glycerol, and 1 mM dithiothreitol. For competition experiments, a 50-fold excess of unlabeled oligonucleotide was added to the reaction mixture, and incubation was continued for additional 20 min. $^{32}$P end-labeled double-stranded oligonucleotide was then added and incubated at room temperature for 20 min. For supershift analysis, 1 μg of anti-HNF4α antibody (Santa Cruz Biotechnology) was added to the reaction mixture. DNA-protein complexes were resolved on a 5% polyacrylamide gel in 0.5× Tris borate/EDTA at room temperature, and a dried gel was exposed to a PhosphorImager screen.

**Statistical Analysis.** All of the values were expressed as the mean ± S.D. All of the data were analyzed by the unpaired Student's *t* test for significant differences; $p < 0.05$ was considered significant.

## Results

**Genes Involved in Trp-NAD Metabolism Are Regulated by PPARα and HNF4α.** To understand the regulatory control of Trp-NAD metabolism in rodents by PP chemicals, wild-type (PPARα$^{+/+}$), PPARα-null (PPARα$^{-/-}$), or liver-specific HNF4α-null mice (HNF4α$^{\Delta L}$) and their floxed (HNF4α$^{F/F}$) littermates were fed Wy-14,643, a PPARα agonist. Real-time PCR analysis revealed that in PPARα$^{+/+}$, HNF4α$^{F/F}$, and HNF4α$^{\Delta L}$ mice, but not in PPARα$^{-/-}$ mice, the expression of peroxisomal acyl-CoA oxidase (ACOX) mRNA was up-regulated by Wy-14,643 (Fig. 2A). These results were in agreement with the fact that *Acox* is a prototypical PPARα target gene. On the other hand, mRNA encoding *Acmsd*, one of the key enzymes involved in Trp-NAD metabolism, was down-regulated by administration of Wy-14,643 in livers of PPARα$^{+/+}$ mice and in both HNF4α$^{F/F}$ and HNF4α$^{\Delta L}$ mice, but not in PPARα$^{-/-}$ mice; the increased expression in the latter mice could be caused by the elevated hepatic HNF4α protein (see below, Fig. 6). However, ACMSD mRNA expression levels in all of the samples were very low compared with the other mRNAs examined. Under control diets, PPARα$^{-/-}$ mice exhibited higher expression levels of ACMSD mRNA than PPARα$^{+/+}$ mice, whereas the HNF4α$^{\Delta L}$ mice exhibited lower expression compared with the HNF4α$^{F/F}$ mice. These results suggest that HNF4α and PPARα regulate ACMSD expression positively and negatively, respectively. Gene expression patterns of QAPRT and TDO mRNA were similar and not substantially affected by Wy-14,643 treatment. There was a small but statistically significant lower QAPRT mRNA in PPARα$^{+/+}$ mice after Wy-14,643 treatment that was not observed in the HNF4α$^{\Delta L}$ mice; we have no explanation for this discrepancy other than possible strain differences. In HNF4α$^{\Delta L}$ mice, however, the expression of these two genes was down-regulated; in particular, QAPRT mRNA was markedly lower compared with HNF4α$^{F/F}$ mice. These results suggest that the expression of *Qaprt* and *Tdo2* may be regulated by HNF4α, but not by PPARα. When ACMSD enzyme activities were examined, a pattern similar to mRNA expression was obtained in either genotype with or without Wy-14,643 (Fig. 2B). A suppression of ACMSD activity in PPARα$^{+/+}$ mice and increased activity in PPARα$^{-/-}$ mice was observed on Wy-14,643 treatment. In the case of HNF4α$^{F/F}$ mice, however, the reduction of enzyme activity was similar to the mRNA levels, but not significantly different in Wy-14,643-treated HNF4α$^{F/F}$ mice, suggesting that the difference may be caused by the shorter period of

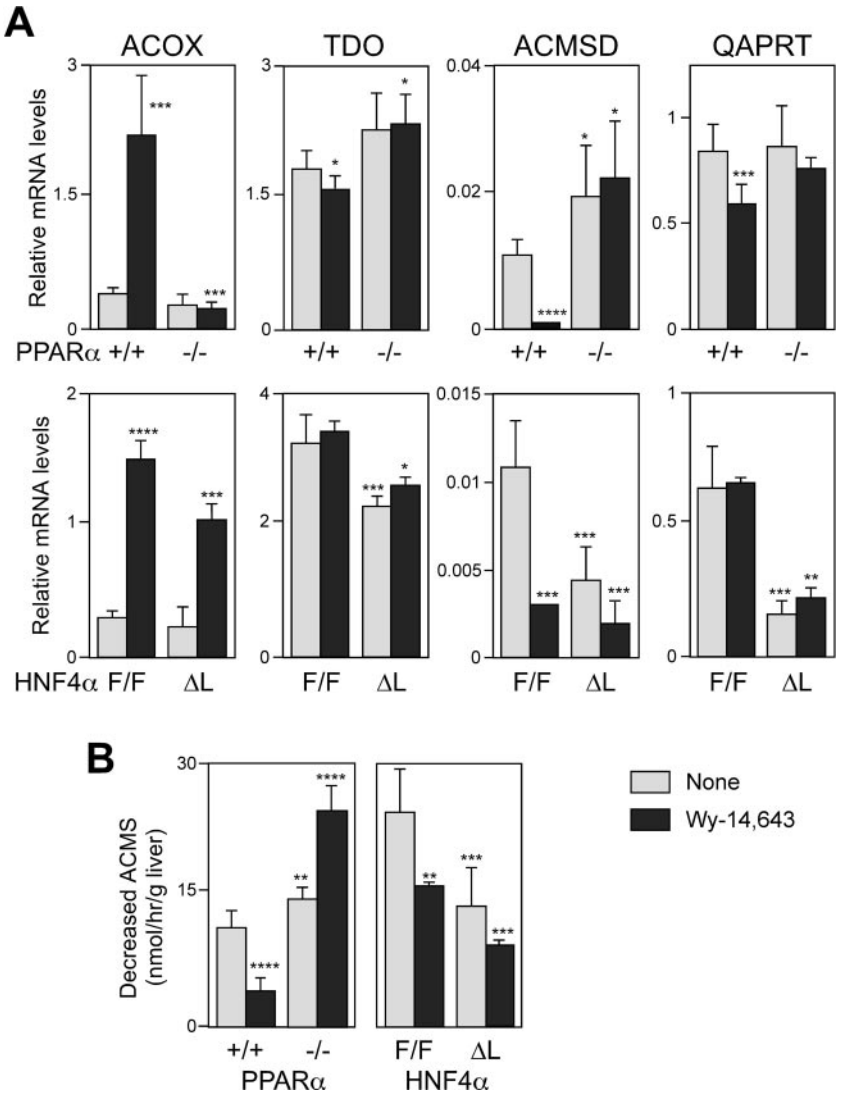


**Fig. 2.** Hepatic mRNA levels of genes related to Trp-NAD metabolism (A) and ACMSD activity (B) in the PPARα$^{-/-}$, PPARα$^{+/+}$, liver-specifically HNF4α-disrupted (HNF4α$^{\Delta L}$), and HNF4α$^{F/F}$ mice fed control or Wy-14,643-containing (0.1%, w/w) diet. A, total RNA extracted from livers of these mice were subjected to real-time PCR analysis, and the results are shown as a relative expression to ribosomal protein 36B4 mRNA levels as normalization control. B, ACMSD activity is shown as the decreased ACMS amount/h in assay condition. Data are expressed as the mean ± S.D. ($n = 5$ for PPARα$^{-/-}$, PPARα$^{+/+}$, and HNF4α$^{F/F}$ mice and $n = 3$ for HNF4α$^{\Delta L}$ mice). Significant differences were based on the values with wild-type mice fed control diet. ****, $p < 0.001$; ***, $p < 0.005$; **, $p < 0.01$; *, $p < 0.05$.

Wy-14,643 dosing. In the following experiments, the regulation of ACMSD by HNF4α and PPARα was examined in more detail.

**Determination of the Transcription Start Site of the Mouse *Acmsd* Gene.** To understand whether the *Acmsd* gene is transcriptionally regulated by HNF4α or PPARα, a DNA fragment containing the 5′-flanking region of the mouse *Acmsd* gene was isolated and the transcription start site determined by 5′-RACE. Two major start sites were identified: one at −74 base pair (bp) and the other at −53 bp upstream from the translation start site. The RACE product with the −74 bp as a start site was found at a higher level (54%) compared with the −53-bp (35%) product. Thus, the former fragment was determined to represent the major transcription start site. Moreover, a TATA motif (TAAA) was located at −28 bp from the −74-bp transcription start site. Therefore, the −74 bp from the translation start site was determined to be the major transcription initiation point of the mouse *Acmsd* gene (Fig. 3).

**HNF4α Activates the Mouse ACMSD Promoter.** Because *Acmsd* gene expression seems to be regulated by both HNF4α and PPARα, the *Acmsd* gene promoter sequence was analyzed for potential consensus binding sites for these transcription factors. Several putative binding sites were identified by MOTIF search (http://motif.genome.jp) with scores higher than 70 for HNF4α within −690 bp upstream of the mouse *Acmsd* gene transcription start site. Although no high-score PPARα binding sites were found, one low-score site was found that partially overlapped with a −224- to −243-bp HNF4α binding site (Fig. 3). Based on this information, several ACMSD promoter-luciferase reporter plasmids were constructed (Fig. 3 and Fig. 4A) and subjected to transient transfection analysis using human hepatocellular carcinoma-derived HepG2 cells that express endogenous HNF4α (Inoue et al., 2002) (Fig. 4B, top). The promoter activity of constructs with −295- and −685-bp fragments was significantly higher than those with the −52- or −220-bp fragment. These results suggested that one or more elements important for hepatic transcription of *Acmsd* gene are located between −295 and −220 bp of the *Acmsd* gene promoter. In fact, a proximal HNF4α binding site was located at −224 to −243 bp of the *Acmsd* gene promoter. Next, monkey kidney-derived CV-1 cells that do not express endogenous HNF4α (Inoue et al., 2002) were used for cotransfection analysis (Fig. 4C, top). In these cells, cotransfection with an HNF4α expression plasmid significantly increased promoter activity of the −295- and −685-bp construct, but promoter activity of the −685-bp construct never exceeded the activity of the −295-bp construct. Cotransfection of these constructs with an HNF1α expression vector had no effect on this promoter activity (data not shown). These results suggest that the putative HNF4α binding site at −224- to −243-bp identified by MOTIF may be responsible for the increased promoter activity.

**Identification of HNF4α Binding Site in the Mouse ACMSD Promoter.** To prove that the putative HNF4α binding site located at −224 to −243 bp directly binds to HNF4α, leading to the transcriptional activation of *Acmsd* gene, electrophoretic mobility shift assays (EMSA) were performed (Fig. 5). The protein in hepatic nuclear extracts from HNF4α$^{F/F}$ mice bound to the ACMSD-HNF4α binding sequence (Fig. 5B, lanes 3 and 6), and the shifted band corresponded in mobility to a band obtained when an HNF4α-consensus sequence was used as a probe (Fig. 5B, lane 1 versus 3). Both bands obtained with the HNF4α-consensus and ACMSD-HNF4α binding sequence were supershifted by the addition of HNF4α antibody (Fig. 5B, lanes 2, 5, and 7). The ACMSD-HNF4α band was completely lost by the addition of a 50-fold molar excess of unlabeled probe (Fig. 5B, lanes 4 and 8; Fig. 5D, lane 18) and by the HNF4α consensus sequence probe (Fig. 5D, lane 19). Furthermore, this band was not detected with extracts from HNF4α$^{\Delta L}$ mouse liver nuclei (Fig. 5B, lanes 9 and 10). Another putative HNF4α binding site with a score higher than 60 located between −685 and −220 bp of the ACMSD promoter did not bind to HNF4α (data not shown).

To confirm that the −224- to −243-bp HNF4α binding site is functionally active, three different mutations were introduced to disrupt binding (Fig. 4A), and EMSA (Fig. 5C) and transfection assays (Fig. 4, B and C) were performed. When

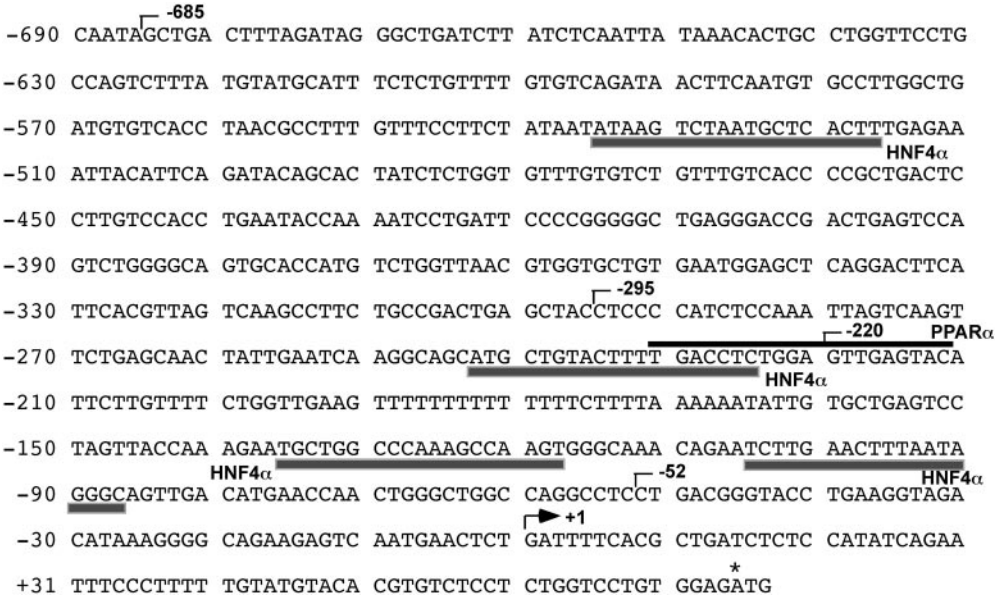


**Fig. 3.** Nucleotide sequence of the mouse *Acmsd* promoter. Numbering of nucleotides is based on the transcription start site as +1 (arrow). Translational start site is marked with asterisk. Several putative HNF4α binding sites and a PPARα binding site with low score that overlaps with the −224- to −243-bp HNF4α binding site are indicated. The nucleotide position of luciferase constructs used for transfection analysis in Fig. 4 is also shown.

examined by EMSA, these mutated probes did not seem to bind to HNF4α (Fig. 5C, lanes 7, 9, and 11), nor did they compete with the ACMSD-HNF4α probe by the addition of unlabeled competitor oligonucleotide probes (Fig. 5C, lanes 4–6). However, a very faint band corresponding in mobility to the HNF4α antibody supershifted band (Fig. 5C, lane 2) was detected with the m1 oligo (Fig. 5C, lane 8), suggesting that this oligo might still have low affinity binding to HNF4α. In the reporter gene assay, in all of the mutated constructs, the increased ACMSD promoter activity observed with HNF4α decreased to levels of activity obtained with the pGL3-basic in both HepG2 and CV-1 cells (Fig. 4B, bottom and Fig. 4C, bottom, respectively). These results show that HNF4α binds to the −224- to −243-bp binding site and increases promoter activity of the ACMSD.

Because a low-score putative PPARα binding site (−212 to −231 bp) is present that partially overlaps with the −224- to −243-bp HNF4α binding site in the *Acmsd* gene promoter, EMSA was carried out to examine whether PPARα binds to this binding site. With an ACOX-peroxisome-proliferator responsive element (PPRE) sequence as a probe and nuclear extracts prepared from PPARα$^{+/+}$ in the presence of Wy-14,643 (Fig. 5D, lanes 3–5), HNF4α$^{F/F}$ in the presence of Wy-14,643 (Fig. 5D, lanes 6 and 7), or PPARα$^{-/-}$ fed control diet (Fig. 5D, lane 8), a clear shifted band was obtained that corresponded to HNF4α (Fig. 5D, lanes 3, 6, and 8 versus 1); this band was lost by the addition of a 50-fold excess of unlabeled oligonucleotide (Fig. 5D, lanes 4 and 7) or the ACMSD-HNF4α oligonucleotide (Fig. 5D, lane 5). Indeed, the ACOX-PPRE contains a sequence similar to the consensus HNF4α binding site (Fig. 5A), thus accounting for this result (Sladek, 1994). When ACMSD-HNF4α was used as a probe with HNF4α$^{F/F}$ nuclear extracts, a shifted band corresponding to HNF4α was lost with a 50-fold excess of unlabeled probes of ACMSD-HNF4α, HNF4α-consensus, or ACOX-PPRE (Fig. 5D, lanes 18, 19, and 22, respectively), but not with ACMSD-PPRE or a consensus PPRE (Fig. 5D, lanes 20 and 21). Furthermore, with the ACMSD-PPRE sequence as a probe, no bands were obtained with any nuclear extracts (Fig. 5D, lanes 9–15). These results suggest that ACMSD-HNF4α sequence does not compete with ACMSD-PPRE sequence and that PPARα may not directly bind the ACMSD-PPRE site located −212 to −231 bp of the ACMSD promoter.

**HNF4α Protein Level Is Decreased in Livers from Mice Treated with Wy-14,643.** To further investigate the mechanism by which PPARα represses the transcription of *Acmsd*, the effect of Wy-14,643 and/or PPARα on the expression of HNF4α in mouse liver was studied by Western blot analysis (Fig. 6A). The chromatin protein HMGB1 (Bustin,

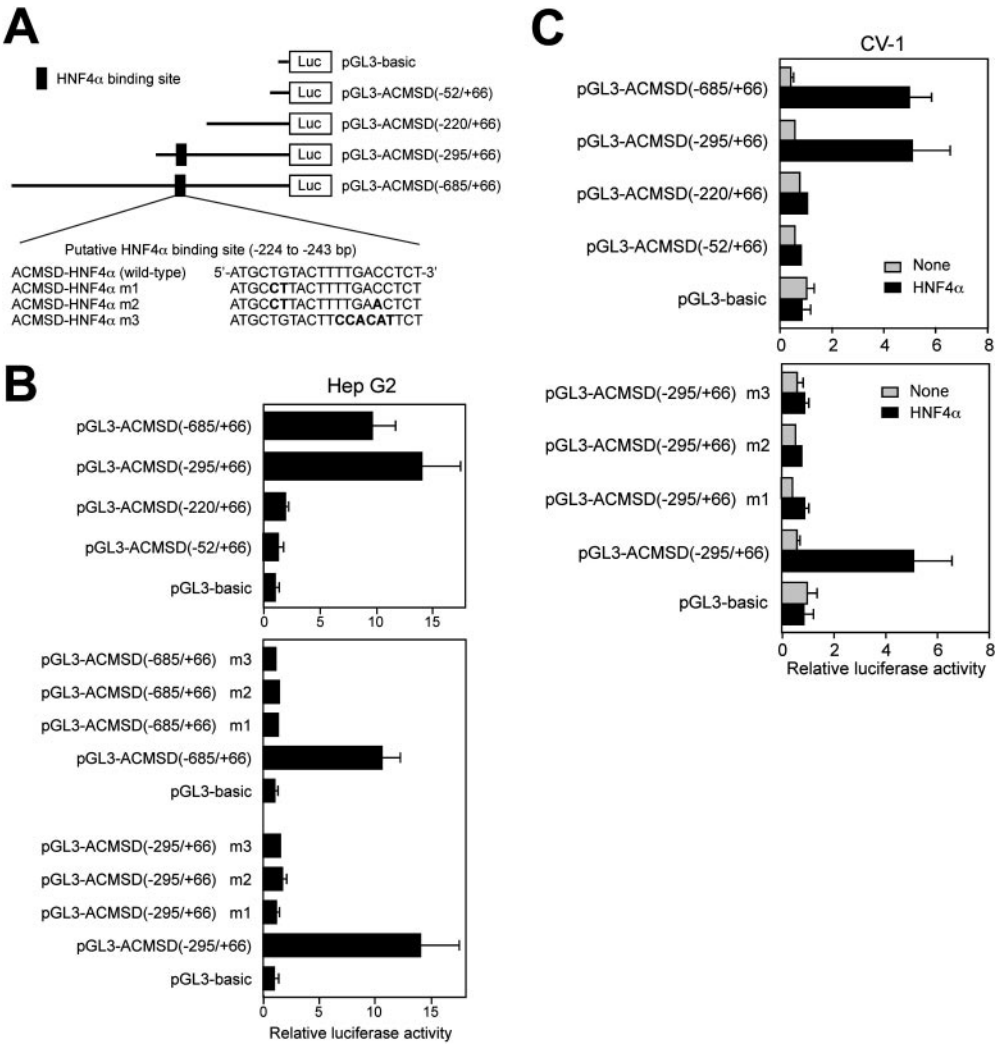


**Fig. 4.** Transfection analysis of mouse ACMSD promoter activity. A, schematic diagram of five luciferase constructs containing various lengths of mouse *Acmsd* promoter sequence (−685, −295, −220, and −52/+66 bp from the transcription start site) used for the analysis. Mutations (m1, m2, m3) introduced into the −224- to −243-bp putative HNF4α binding site (ACMSD-HNF4α) are also shown. B, *Acmsd* promoter activities obtained by transfecting five *Acmsd* reporter constructs (top) and the mutated constructs of −685 and −295, each containing m1, m2, or m3 mutation (bottom) into HepG2 cells. C, cotransfection analysis of five *Acmsd* reporter constructs (top) and −295 constructs containing m1, m2, or m3 mutation (bottom) with and without HNF4α expression plasmid in CV-1 cells. All of the values are expressed as -fold induction based on the activity obtained with the pGL3-basic plasmid as 1. Data are the mean ± S.D. from three separate experiments, each done in triplicate.

2002) and GAPDH were used as controls for nuclear and cytoplasmic proteins, respectively. Interestingly, HNF4α protein level was decreased in livers of Wy-14,643-treated PPARα$^{+/+}$ and HNF4α$^{F/F}$ mice but not PPARα$^{-/-}$ livers; the latter mice had increased levels of HNF4α compared with PPARα$^{+/+}$ with and without Wy-14,643 treatment. The reason for this increase is not known, but it is correlated with the increase in ACMSD mRNA in the livers of PPARα$^{-/-}$ mice (Fig. 2A). As expected, no HNF4α protein was detected in HNF4α$^{\Delta L}$ liver. Mature OTC located in mitochondria and a positive control product for a bonafide HNF4α target gene also showed decreased amounts after Wy-14,643 treatment in both PPARα$^{+/+}$ and HNF4α$^{F/F}$ mice. This protein was not detected in the extract from HNF4α$^{\Delta L}$ mouse liver. These data suggest that the decreased protein level of OTC may be caused by the lower hepatic levels of HNF4α protein.

The effect of Wy-14,643 on HNF4α mRNA levels and its target genes was also examined by Northern blotting (Fig. 6B). Levels of PPARα mRNA increased in livers of PPARα$^{+/+}$, HNF4α$^{F/F}$, and HNF4α$^{\Delta L}$ mice treated with Wy-14,643. ACOX mRNA was also markedly induced in these mice. HNF4α mRNA levels were similar with or without Wy-14,643 in PPARα$^{+/+}$ and HNF4α$^{F/F}$ mouse livers, in contrast to the results found with protein expression. However, the expression of several HNF4α target genes, such as *Otc*, liver-type pyruvate kinase *Pklr*), and apolipoprotein C-III (*ApoC3*) was significantly decreased in the liver of PPARα$^{+/+}$ and HNF4α$^{F/F}$ mice treated with Wy-14,643, but not PPARα$^{-/-}$ mice, suggesting that the decrease in expression of these genes is PPARα-dependent. Taken together, these results show that Wy-14,643, through PPARα, regulates HNF4α levels post-transcriptionally, resulting in decreased expression of HNF4α target genes, including *Acmsd*, by decreasing the cellular levels of HNF4α.

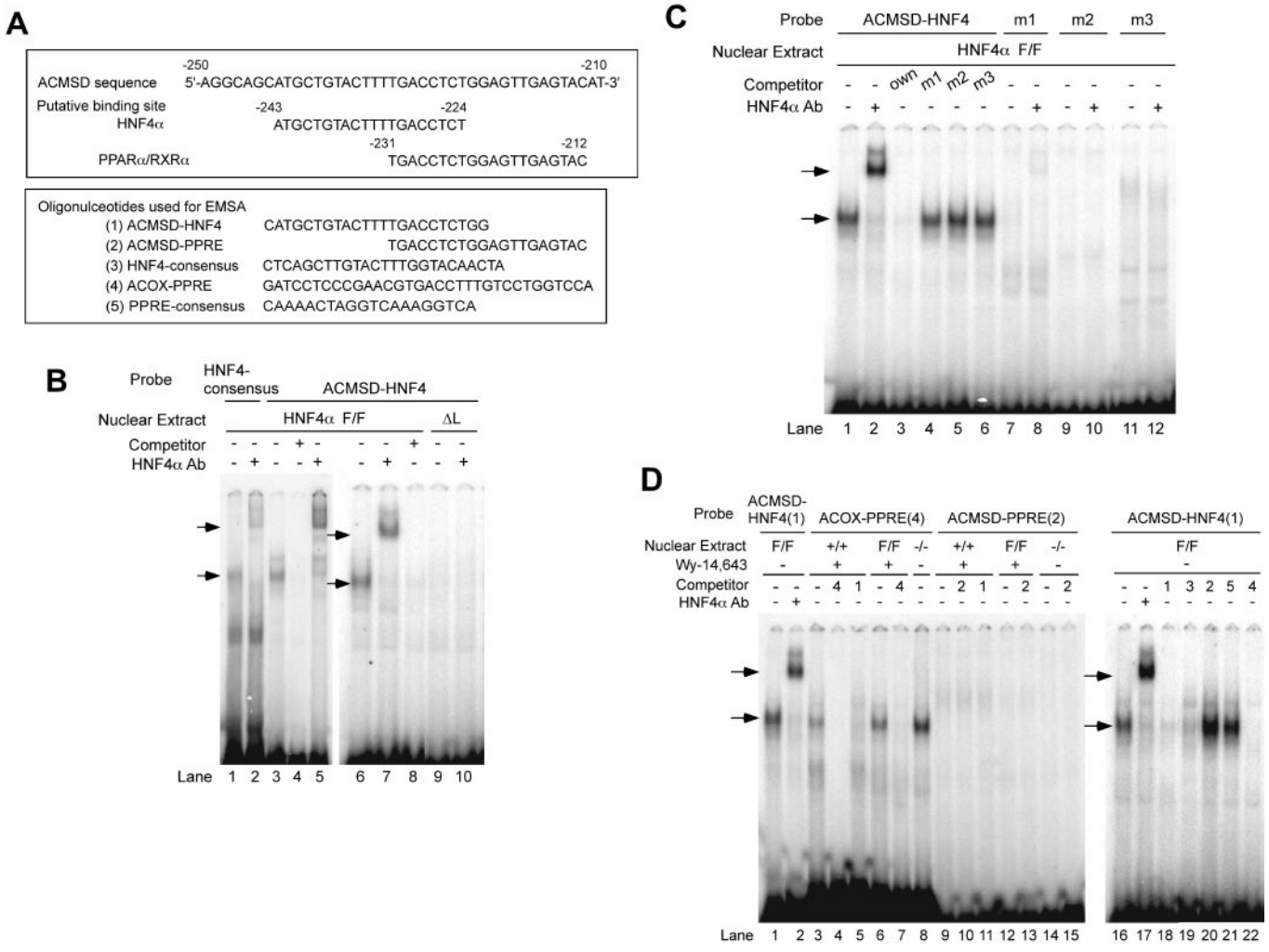


**Fig. 5.** Examination of HNF4α and PPARα binding sites in the mouse *Acmsd* promoter by EMSA. A, list of sequences used for EMSA experiments. B, nuclear extracts from the liver of HNF4α$^{F/F}$ (lanes 1–8) or HNF4α$^{\Delta L}$ mice (lanes 9 and 10) were incubated with labeled HNF4-consensus (lanes 1 and 2) or ACMSD-HNF4 probe (lanes 3–10); lanes 4 and 8 in the presence of excess unlabeled ACMSD-HNF4 oligonucleotide, and lanes 2, 5, 7, and 10 with the addition of anti-HNF4α antibody. C, the effect of mutation introduced into the HNF4α binding site was examined using ACMSD-HNF4 as a probe and the following sequences as competitors: own oligonucleotide (lane 3), m1 (lane 4), m2 (lane 5), and m3 (lane 6) (see Fig. 4A). Lanes 7 through 12, oligonucleotides m1 (lanes 7 and 8), m2 (lanes 9 and 10), and m3 (lanes 11 and 12) were also used as a probe. Nuclear extracts from the liver of HNF4α$^{F/F}$ were used for all of the lanes. D, ACMSD-HNF4 (lanes 1, 2, and 16–22), ACOX-PPRE (lanes 3–8), and ACMSD-PPRE sequence (lanes 9–15) were used as a probe for EMSA with the following competitors; ACMSD-HNF4 own oligonucleotide (1) (lanes 5, 11, and 18), ACOX-PPRE (4) (lanes 4, 7, and 22), ACMSD-PPRE (2) (lanes 10, 13, 15, and 20), HNF4-consensus (3) (lane 19), or PPRE-consensus (5) (lane 21). Nuclear extracts from the liver of HNF4α$^{F/F}$, control diet (lanes 1, 2, and 16–22), HNF4α$^{F/F}$, Wy-14,643 diet (lanes 6, 7, 12, and 13), PPARα$^{+/+}$, Wy-14,643 diet (lanes 3–5 and 9–11), and PPARα$^{-/-}$, control diet (lanes 8, 14, and 15) were used. An arrow denotes the HNF4α-specific band and its supershifted band.

## Discussion

ACMSD and QAPRT are the key enzymes in Trp-NAD metabolism and regulate the flux to NAD from Trp in rodents. Alteration in ACMSD activity is correlated with hepatic NAD levels (Shin et al., 1999) and the NAD metabolites $N^1$-methylnicotinamide, $N^1$-methyl-4-pyridone-3-carboxamide, and $N^1$-methyl-2-pyridone-5-carboxamide excreted in urine as biomarkers (Delaney et al., 2005). ACMSD activity was reported to be down-regulated by dietary PUFA (Egashira et al., 2004), low protein (Fukuoka et al., 2002), and PP (Loo et al., 1995; Shin et al., 1999) and up-regulated by glucocorticoids (Fukuoka et al., 2002), high protein diets, and in streptozotocin-induced diabetic rats (Tanabe et al., 2002). The mechanisms mediating these activity changes are not known.

By using PPARα-null or liver-specific HNF4α-null mice in the current study, the expression of ACMSD was found to be under positive and negative regulation of HNF4α and PPARα, respectively. ACMSD mRNA is suppressed in wild-type mice and not in PPARα-null mice administered the ligand Wy-14,643, indicating that PPARα attenuates *Acmsd* gene expression. Levels of ACMSD mRNA and activity are markedly lower in mice lacking hepatic expression of HNF4α, revealing that HNF4α controls constitutive expression of the gene. Indeed, a functional HNF4α binding site was located in the ACMSD gene promoter that is responsible for the increased promoter activity by HNF4α as assessed by reporter gene transfection studies. Activation of PPARα also results in post-transcriptional suppression of HNF4α protein levels that correlates with decreased expression of ACMSD. However, ACMSD expression is also suppressed in HNF4α$^{\Delta L}$ mice fed Wy-14,643, suggesting that there may be another indirect mechanism by which this gene is suppressed by PPARα. HNF4α is constitutively expressed in liver and is active in the absence of exogenous ligand, whereas PPARα is a ligand-activated transcription factor. HNF4α and PPARα share similar hexanucleotide direct repeat 1 (DR1) consensus binding sequences (Sladek, 1994; Hertz et al., 1998). Indeed, a DR1 was found in the mouse *Acmsd* promoter, and activation of the promoter was mediated by HNF4α binding similar to other HNF4α target genes (Rajas et al., 2002). DR1 elements are quite promiscuous, thus allowing binding of other transcription factors, including HNF4α, PPARα/RXRα, RXRα homodimers, retinoic acid receptor α/RXRα heterodimers, and chicken ovalbumin upstream promoter transcription factor I and II (Nakshatri and Bhat-Nakshatri, 1998), suggesting that these factors potentially could compete for binding to specific DR1 elements. Competitive binding of HNF4α and PPARα/RXRα to DR1 elements as a mechanism for modulating transcriptional activation of target genes has been proposed (Hertz et al., 1995, 1996; Marrapodi and Chiang, 2000). For example, HNF4α was reported to bind to the ACOX-PPRE (Sladek, 1994), and in HepG2 cells, the apoC-III promoter activity was affected by hypolipidemic drugs (Hertz et al., 1995). PPARα and RXRα specifically counteracted HNF4α-activated transcription rather than inhibiting basal transcription of apoC-III. This result is similar to what was observed for the *Acmsd* gene in the current study. By EMSA using in vitro translated or COS cell-expressed transcription factors, HNF4α and PPARα/RXRα heterodimers bound strongly to the C3P elements (Hertz et al., 1995), previously shown to be the binding site of nuclear proteins to the rat and human apoC-III gene promoter (Ladias et al., 1992, Mietus-Snyder et al., 1992). However, the binding of PPARα/RXRα to the *Acmsd* gene HNF4α binding site was not observed in the current studies. These data indicate that PPARα reduces *Acmsd* gene expression indirectly through decreasing cellular contents of HNF4α protein. However, it should be noted that a small but significant suppression of residual ACMSD activity was also found in the HNF4α$^{\Delta L}$ liver fed Wy-14,643, suggesting the possibility of another mechanism for attenuation of expression in this mouse model that is independent of HNF4α protein. In another study, cholesterol 7α-hydroxylase was reduced by treatment with fibrates, and the reporter activity of a human cholesterol 7α-hydroxylase-luciferase construct was down-regulated by Wy-14,643 (Marrapodi and Chiang, 2000). Similar to the current results with *Acmsd*, no direct binding of in vitro synthesized PPARα/RXRα heterodimer to the DR1 element of this gene was detected by EMSA. Therefore, it was suggested that attenuation of the transactivation of this gene is caused by altered availability of HNF4α in the presence of PPARα and its ligand (Marrapodi and Chiang, 2000). The

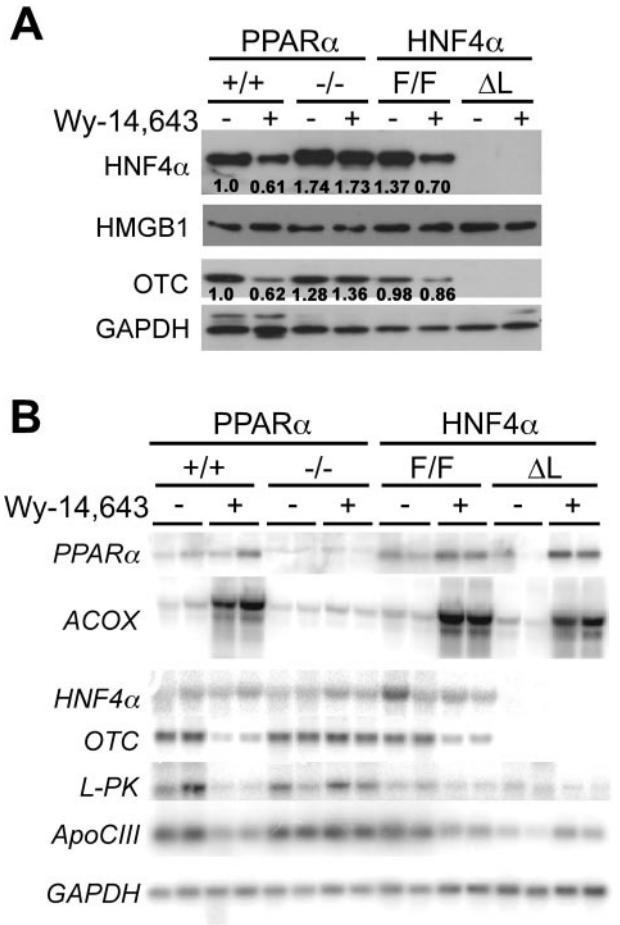


**Fig. 6.** Protein and mRNA levels of HNF4α, PPARα, and/or their target genes. A, Western blot analysis of HNF4α protein levels in the nuclear extract of livers from PPARα$^{+/+}$, PPARα$^{-/-}$, HNF4α$^{F/F}$, and HNF4α$^{\Delta L}$ mice fed control or Wy-14,643 diet. HMGB1 (33) and GAPDH were used as loading controls for nuclear and non-nuclear fractions, respectively. The quantitated ratios of HNF4α/HMGB1 and HNF4α/OTC, with the PPARα$^{+/+}$ set at 1.0, are shown. B, Northern blot analysis of RNA obtained from the same mice livers used for A. ACOX is a PPARα target gene. OTC, L-PK, and apoCIII are HNF4α target genes.

effects of fibrates on HNF4α protein were not examined in this study.

The current finding, that Wy-14,643 treatment resulted in a PPARα-dependent suppression of HNF4α protein levels, is similar to that observed in HepG2 cells treated with Wy-14,643 (Marrapodi and Chiang, 2000). Of interest, activation of AMP-activated protein kinase (AMPK) by 5-amino-4-imidazolecarboxamide riboside in hepatocytes decreased HNF4α protein levels, and consequently the expression of HNF4α target genes was down-regulated, but HNF4α mRNA was unchanged (Leclerc et al., 2001). Indeed, in the liver of $PPAR^{+/+}$ and $HNF4\alpha^{F/F}$ mice treated with Wy-14,643, expression of HNF4α target genes encoding *Otc1*, *Pklr*, and *ApoC3* were also down-regulated. Phosphorylation was suggested to be one of regulatory mechanisms of HNF4α transactivation activity. HNF4α can be phosphorylated by protein kinase A (Viollet et al., 1997), extracellular signal-regulated kinase (Reddy et al., 1999), AMPK (Leclerc et al., 2001; Hong et al., 2003), and c-Jun $NH_2$-terminal kinase 1 (Jahan and Chiang, 2005), and phosphorylation suppresses the DNA-binding affinity and *trans*-activation of HNF4α. Modulation of kinase activity can also alter target gene expression by altering HNF4α protein levels (Reddy et al., 1999; Leclerc et al., 2001; Hong et al., 2003; Jahan and Chiang, 2005). Inhibition of extracellular signal-regulated kinase increased HNF4α mRNA and protein level (Reddy et al., 1999), whereas activation of AMPK was shown to promote degradation of HNF4α protein without changing HNF4α mRNA expression (Leclerc et al., 2001; Hong et al., 2003). However, preliminary studies in vivo revealed that activation of PPARα by Wy-14,643 had no effect on AMPK activity (date now shown). In any case, it still remains to be determined whether phosphorylation is the underlying mechanism of the reduced HNF4α protein level and ACMSD expression in Wy-14,643-treated mouse liver, and which kinase is responsible. Nevertheless, it is interesting that the activation of PPARα represses HNF4α protein expression, as well as transcription of its target genes, suggesting that some phenotypes resulting from PPARα activation in liver may be through HNF4α repression. Given that PPARα target gene expression was induced in HNF4α-null mouse liver (Hayhurst et al., 2001), it is of interest to investigate cross-talk between PPARα and HNF4α in normal and disease states.

In conclusion, the role of transcriptional factors HNF4α and PPARα in the biosynthesis of Trp-NAD was examined. The ACMSD promoter activity was found to be under direct transcriptional regulation by HNF4α. Wy-14,643 activation of PPARα indirectly results in suppression of HNF4α protein levels, leading to the negative regulation of ACMSD activity. These results will provide a better understanding of the Trp-NAD pathway and NAD homeostasis.

**Acknowledgments**

We thank Connie Cheung, Masamichi Yamashita, Keiichirou Morimura, and Yatrik Shah for providing animals and technical advice.

**References**

Bender DA (1983) Biochemistry of tryptophan in health and disease. *Mol Aspects Med* **6:**101–197.

Bustin M (2002) At the crossroads of necrosis and apoptosis: signaling to multiple cellular targets by HMGB1. *Sci STKE* **2002:**PE39.

Delaney J, Hodson MP, Thakkar H, Connor SC, Sweatman BC, Kenny SP, McGill PJ, Holder JC, Hutton KA, Haselden JN, et al. (2005) Tryptophan-$NAD^+$ pathway metabolites as putative biomarkers and predictors of peroxisome proliferation. *Arch Toxicol* **79:**208–223.

Egashira Y, Murotani G, Tanabe A, Saito K, Uehara K, Morise A, Sato M, and Sanada H (2004) Differential effects of dietary fatty acids on rat liver alpha-amino-beta-carboxymuconate-epsilon-semialdehyde decarboxylase activity and gene expression. *Biochim Biophys Acta* **1686:**118–124.

Fukuoka S, Ishiguro K, Yanagihara K, Tanabe A, Egashira Y, Sanada H, and Shibata K (2002) Identification and expression of a cDNA encoding human alpha-amino-beta-carboxymuconate-epsilon-semialdehyde decarboxylase (ACMSD). A key enzyme for the tryptophan-niacine pathway and "quinolinate hypothesis." *J Biol Chem* **277:**35162–35167.

Hayhurst GP, Lee YH, Lambert G, Ward JM, and Gonzalez FJ (2001) Hepatocyte nuclear factor 4alpha (nuclear receptor 2A1) is essential for maintenance of hepatic gene expression and lipid homeostasis. *Mol Cell Biol* **21:**1393–1403.

Hertz R, Bishara-Shieban J, and Bar-Tana J (1995) Mode of action of peroxisome proliferators as hypolipidemic drugs. Suppression of apolipoprotein C-III. *J Biol Chem* **270:**13470–13475.

Hertz R, Magenheim J, Berman I, and Bar-Tana J (1998) Fatty acyl-CoA thioesters are ligands of hepatic nuclear factor-4alpha. *Nature (Lond)* **392:**512–516.

Hertz R, Seckbach M, Zakin MM, and Bar-Tana J (1996) Transcriptional suppression of the transferrin gene by hypolipidemic peroxisome proliferators. *J Biol Chem* **271:**218–224.

Hertz R, Sheena V, Kalderon B, Berman I, and Bar-Tana J (2001) Suppression of hepatocyte nuclear factor-4alpha by acyl-CoA thioesters of hypolipidemic peroxisome proliferators. *Biochem Pharmacol* **61:**1057–1062.

Hong YH, Varanasi US, Yang W, and Leff T (2003) AMP-activated protein kinase regulates HNF4α transcriptional activity by inhibiting dimer formation and decreasing protein stability. *J Biol Chem* **278:**27495–27501.

Hostetler HA, Petrescu AD, Kier AB, and Schroeder F (2005) Peroxisome proliferator-activated receptor α interacts with high affinity and is conformationally responsive to endogenous ligands. *J Biol Chem* **280:**18667–18682.

Ikeda M, Tsuji H, Nakamura S, Ichiyama A, Nishizuka Y, and Hayaishi O (1965) Studies on the biosynthesis of nicotinamide adenine dinucleotide. II. A role of picolinic carboxylase in the biosynthesis of nicotinamide adenine dinucleotide from tryptophan in mammals. *J Biol Chem* **240:**1395–1401.

Inoue Y, Hayhurst GP, Inoue J, Mori M, and Gonzalez FJ (2002) Defective ureagenesis in mice carrying a liver-specific disruption of hepatocyte nuclear factor 4alpha (HNF4alpha). HNF4α regulates ornithine transcarbamylase in vivo. *J Biol Chem* **277:**25257–25265.

Inoue Y, Peters LL, Yim SH, Inoue J, and Gonzalez FJ (2006a) Role of hepatocyte nuclear factor 4alpha in control of blood coagulation factor gene expression. *J Mol Med* **84:**334–344.

Inoue Y, Yu A, Yim SH, Ma X, Krausz KW, Inoue J, Xiang CC, Brownstein ML, Eggertsen G, Björkhem I, et al. (2006b) Regulation of bile acid synthesis by hepatocyte nuclear factor 4α. *J Lipid Res* **7:**215–227.

Jahan A and Chiang JY (2005) Cytokine regulation of human sterol 12alpha-hydroxylase (CYP8B1) gene. *Am J Physiol* **288:**G685–G695.

Jump DB (2002) Dietary polyunsaturated fatty acids and regulation of gene transcription. *Curr Opin Lipidol* **13:**155–164.

Jump DB, Thelen A, and Mater M (1999) Dietary polyunsaturated fatty acids and hepatic gene expression. *Lipids* **34 (Suppl):**S209–S212.

Kamiya A, Inoue Y, Kodama T, and Gonzalez FJ (2004) Hepatocyte nuclear factors 1alpha and 4alpha control expression of proline oxidase in adult liver. *FEBS Lett* **578:**63–68.

Ladias JA, Hadzopoulou-Cladaras M, Kardassis D, Cardot P, Cheng J, Zannis V, and Cladaras C (1992) Transcriptional regulation of human apolipoprotein genes ApoB, ApoCIII, and ApoAII by members of the steroid hormone receptor superfamily HNF-4, ARP-1, EAR-2, and EAR-3. *J Biol Chem* **267:**15849–15860.

Leclerc I, Lenzner C, Gourdon L, Vaulont S, Kahn A, and Viollet B (2001) Hepatocyte nuclear factor-4alpha involved in type 1 maturity-onset diabetes of the young is a novel target of AMP-activated protein kinase. *Diabetes* **50:**1515–1521.

Lee SS, Pineau T, Drago J, Lee EJ, Owens JW, Kroetz DL, Fernandez-Salguero PM, Westphal H, and Gonzalez FJ (1995) Targeted disruption of the alpha isoform of the peroxisome proliferator-activated receptor gene in mice results in abolishment of the pleiotropic effects of peroxisome proliferators. *Mol Cell Biol* **15:**3012–3022.

Loo Y, Shin M, Yamashita Y, Ishigami M, Sasaki M, Sano K, and Umezawa C (1995) Effect of feeding clofibrate-containing diet on the hepatic $NAD^+$ level in rats. *J Nutr Sci Vitaminol (Tokyo)* **41:**341–347.

Marrapodi M and Chiang JY (2000) Peroxisome proliferator-activated receptor alpha (PPARalpha) and agonist inhibit cholesterol 7alpha-hydroxylase gene (CYP7A1) transcription. *J Lipid Res* **41:**514–520.

Mehler AH (1956) Formation of picolinic and quinolinic acids following enzymatic oxidation of 3-hydroxyanthranilic acid. *J Biol Chem* **218:**241–254.

Mehler AH, Mc DE, and Hundley JM (1958) Changes in the enzymatic composition of liver. I. Increase of picolinic carboxylase in diabetes. *J Biol Chem* **232:**323–330.

Mietus-Snyder M, Sladek FM, Ginsburg GS, Kuo CF, Ladias JA, Darnell JE Jr, and Karathanasis SK (1992) Antagonism between apolipoprotein AI regulatory protein 1, Ear3/COUP-TF, and hepatocyte nuclear factor 4 modulates apolipoprotein CIII gene expression in liver and intestinal cells. *Mol Cell Biol* **12:**1708–1718.

Nakshatri H and Bhat-Nakshatri P (1998) Multiple parameters determine the specificity of transcriptional response by nuclear receptors HNF-4, ARP-1, PPAR, RAR and RXR through common response elements. *Nucleic Acids Res* **26:**2491–2499.

Pegorier JP, Le May C, and Girard J (2004) Control of gene expression by fatty acids. *J Nutr* **134:**2444S–2449S.

Petrescu AD, Hertz R, Bar-Tana J, Schroeder F, and Kier AB (2002) Ligand specificity and conformational dependence of the hepatic nuclear factor-4α (HNF-4α). *J Biol Chem* **277:**23988–23999.

Rajas F, Gautier A, Bady I, Montano S, and Mithieux G (2002) Polyunsaturated fatty acyl coenzyme A suppress the glucose-6-phosphatase promoter activity by modu-

lating the DNA binding of hepatocyte nuclear factor 4α. *J Biol Chem* **277:**15736–15744.
Reddy S, Yang W, Taylor DG, Shen X, Oxender D, Kust G, and Leff T (1999) Mitogen-activated protein kinase regulates transcription of the ApoCIII gene. Involvement of the orphan nuclear receptor HNF4. *J Biol Chem* **274:**33050–33056.
Rhee J, Inoue Y, Yoon JC, Puigserver P, Fan M, Gonzalez FJ, and Spiegelman BM (2003) Regulation of hepatic fasting response by PPARgamma coactivator-1alpha (PGC-1): requirement for hepatocyte nuclear factor 4alpha in gluconeogenesis. *Proc Natl Acad Sci USA* **100:**4012–4017.
Sanada H and Miyazaki M (1984) Effect of high-protein diet on liver alpha-amino-beta-carboxymuconate-epsilon-semialdehyde decarboxylase in rats. *J Nutr Sci Vitaminol (Tokyo)* **30:**113–123.
Shin M, Mori Y, Kimura A, Fujita Y, Yoshida K, Sano K, and Umezawa C (1996) NAD+ biosynthesis and metabolic fluxes of tryptophan in hepatocytes isolated from rats fed a clofibrate-containing diet. *Biochem Pharmacol* **52:**247–252.
Shin M, Ohnishi M, Iguchi S, Sano K, and Umezawa C (1999) Peroxisome-proliferator regulates key enzymes of the tryptophan-NAD+ pathway. *Toxicol Appl Pharmacol* **158:**71–80.
Sladec F and Seidel SD (2001) Hepatocyte nuclear factor 4alpha, in *Nuclear Receptors and Genetic Disease* (Burris T and McCabe ERB eds) pp 309–361, Academic Press, San Diego.
Sladek F (1994) Hepatocyte nuclear factor 4 (HNF-4), in *Liver Gene Expression* (Trouche F and Yaniv M eds) pp 207–230, R.G. Landers Co., Austin, TX.
Tanabe A, Egashira Y, Fukuoka S, Shibata K, and Sanada H (2002) Expression of rat hepatic 2-amino-3-carboxymuconate-6-semialdehyde decarboxylase is affected by a high protein diet and by streptozotocin-induced diabetes. *J Nutr* **132:**1153–1159.
Viollet B, Kahn A, and Raymondjean M (1997) Protein kinase A-dependent phosphorylation modulates DNA-binding activity of hepatocyte nuclear factor 4. *Mol Cell Biol* **17:**4208–4219.

**Address correspondence to:** Dr. Frank J. Gonzalez, Building 37, Room 3106, National Cancer Institute, National Institutes of Health, Bethesda, MD 20892. E-mail: fjgonz@helix.nih.gov